

*XVII IMEKO World Congress
Metrology in the 3rd Millennium
June 22–27, 2003, Dubrovnik, Croatia*

ADVANCED FEM-3D METROLOGICAL APPROACH TO THE ANALYSIS OF COMBINED INSTRUMENT TRANSFORMER

Marija Cundeva & Ljupco Arsov

University “Sts. Cyril & Methodius”, Faculty of Electrical Engineering, Skopje, R. Macedonia

Abstract – An advanced and novel numerical method for analysis of combined instrument transformer will be given in this paper. The three-dimensional magnetic field analysis results by using the finite element method will be used for estimation of the metrological characteristics of the transformer. The analytical and the results derived by the original FEM-3D program package will be compared and discussed. This will enable further optimal design of the instrument transformer prototype by taking into consideration the exact mutual electromagnetic influence of both transformation cores (current and voltage measurement magnetic cores) and by using stochastic optimisation techniques.

Keywords: Instrument transformer, finite element method

1. INTRODUCTION

The instrument transformers as one of the main components of the power measurement systems should transform the measured voltages and currents with the lowest uncertainty (voltage, current and phase difference errors), [1]. The combined current-voltage instrument transformer is a non-linear electromagnetic system with complex configuration: two measurement transformation cores (voltage and current transformation core) in common housing, with increased metrological errors because of the mutual electromagnetic influence between the two cores, [2]. The analytical expressions for calculation of the magnetic field distribution can be applied for simple electromagnetic systems, [2, 4]. Correct estimation of the metrological parameters of the 20 kV combined instrument transformer (voltage transformation ratio: $20000 \frac{V}{\sqrt{3}} : 100 \frac{V}{\sqrt{3}}$ and current transformation ratio: 100 A : 5 A) can be achieved by using the numerical methods, only [2, 3].

2. FEM-3D MODELLING OF THE COMBINED INSTRUMENT TRANSFORMER

The magnetic field distribution in the instrument transformer is described by the system of Maxwell’s equations. The magnetic vector potential A is an auxiliary quantity, B is the magnetic flux density, v is the magnetic reluctivity

and j is the current density. The magnetic field is modelled by the Poisson’s non-linear differential equation:

$$\frac{\partial}{\partial x} \left(v(B) \frac{\partial A}{\partial x} \right) + \frac{\partial}{\partial y} \left(v(B) \frac{\partial A}{\partial y} \right) + \frac{\partial}{\partial z} \left(v(B) \frac{\partial A}{\partial z} \right) = -j(x, y, z) \quad (1)$$

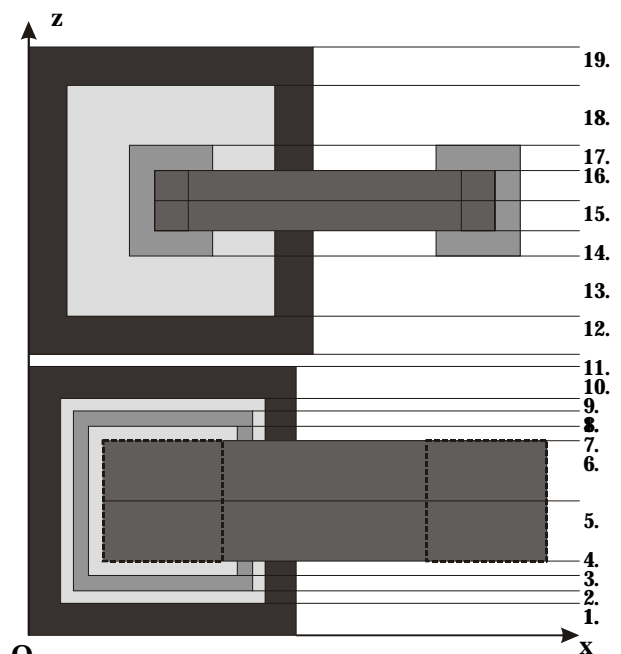


Fig. 1. Electromagnetic system of the combined instrument transformer with the 19 layers along the z-axis of the 3D-domain (vt-voltage transformation, ct-current transformation)

- 1- VT primary winding (down)
- 2- VT isolation (down)
- 3- VT secondary winding (down)
- 4- VT isolation (down)
- 5- VT magnetic core (down)
- 6- VT magnetic core (up)
- 7- VT isolation (up)
- 8- VT secondary winding (up)
- 9- VT isolation (up)
- 10- VT primary winding (up)
- 11- main isolation
- 12- CT primary winding (down)
- 13- CT isolation (down)
- 14- CT secondary winding (down)
- 15- CT magnetic core (down)
- 16- CT magnetic core (up)
- 17- CT secondary winding (up)
- 18- CT isolation (up)
- 19- CT primary winding (up)

The original program package FEM-3D, [3], developed at the Faculty of Electrical Engineering in Skopje is used for calculation of non-linear partial differential equations system (1) with prescribed Dirichlet and Neumann boundary conditions in the nodes of the 19000 finite elements of the combined current-voltage instrument transformer mesh. For proper mathematical and geometrical modelling of the combined transformer the 3D domain is divided into 19 layers along the z-axis, given in Fig. 1.

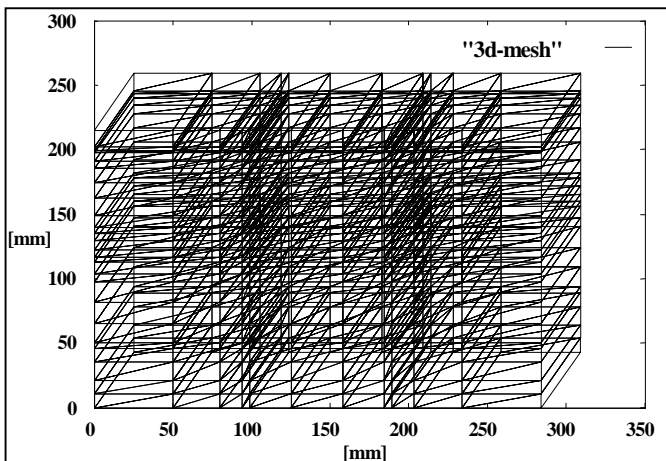


Fig. 2. Finite element mesh in one layer of the 3D domain

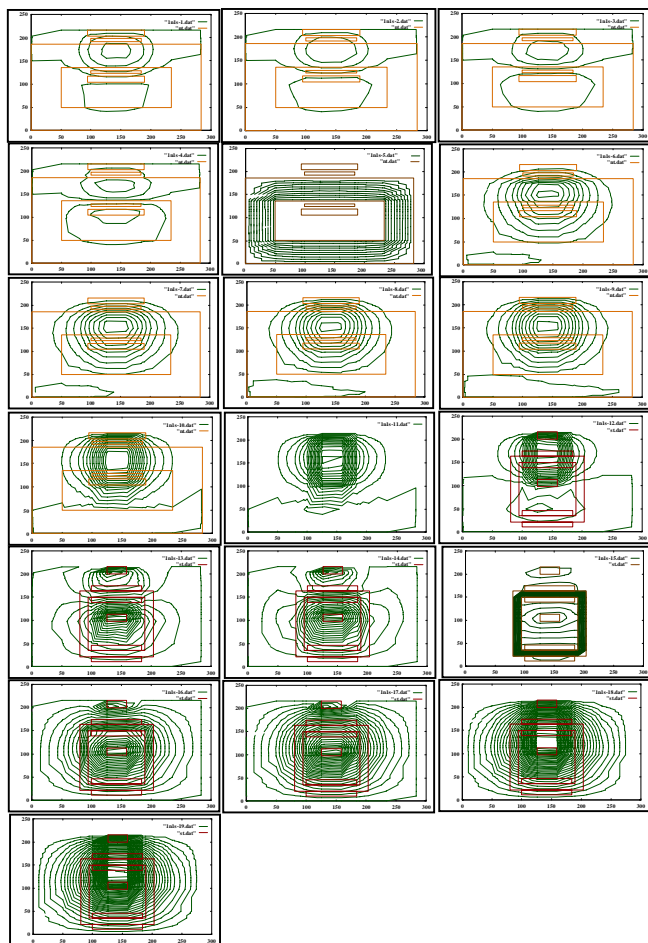


Fig. 3. Flux plots in the 19 cross-sectional layers of the 3D domain

For exact calculation of the leakage fluxes in the air the winding end-regions are taken into consideration. The 3D mesh of finite elements in one layer is displayed at Fig 2.

The magnetic anisotropy and the lamination of the magnetic cores are considered. The Weighted Residual Method is used in the iterative calculator of the FEM-3D package. The non-linear magnetic characteristics of the high quality grain-oriented electrical steel sheet type 27-moh is taken into account. The input values of the voltages and currents are changed from the plug out regime to the stationary state of 120% of their nominal values at constant nominal load ($S_{nv}=50$ VA of the voltage transformation core, $S_{nc}=15$ VA of the current transformation core and $\cos\phi_n=0,8$ of the both cores). The magnetic vector potential A is calculated at the nodes of the finite element mesh. The flux plots in the 19 layers of the combined transformer are shown in Fig. 3. By using the numerical integration the magnetic flux density in different parts of the electromagnetic system is determined. This enables exact calculation of the leakage inductances of the combined transformer four windings.

3. COMPARED ANALYTICAL AND FEM-3D RESULTS

In Table I. the analytical and the FEM-3D derived results of the magnetic flux density in the middle of the voltage transformation magnetic core are given.

TABLE I. Analytically and numerically calculated values of the magnetic flux density B_{mV} in the middle of the VT core

I/I_n	only VT	only VT	0	0,2	0,4	0,6	0,8	1,0	1,2
	analyt.	numerical							
U/U_n	B_{mV} [T]								
0,2	0,18	0,24	0,24	0,17	0,10	0,03	0,04	0,11	0,18
0,4	0,37	0,49	0,49	0,42	0,34	0,27	0,20	0,13	0,06
0,6	0,55	0,72	0,72	0,65	0,58	0,51	0,44	0,37	0,30
0,8	0,73	0,97	0,97	0,90	0,82	0,75	0,68	0,61	0,54
1,0	0,91	1,21	1,21	1,14	1,08	1,00	0,93	0,85	0,78
1,2	1,10	1,46	1,46	1,38	1,31	1,24	1,17	1,10	1,03

In Table II. the analytical and the FEM-3D derived results of the magnetic flux density in the middle of the current transformation magnetic core are given.

TABLE II. Analytically and numerically calculated values of the magnetic flux density B_{mC} in the middle of the CT core

U/U_n	only CT	only CT	0	0,2	0,4	0,6	0,8	1,0	1,2
	analyt.	numerical							
I/I_n	B_{mC} [T]								
0,2	0,07	0,08	0,08	0,08	0,08	0,08	0,08	0,08	0,08
0,4	0,14	0,16	0,16	0,16	0,16	0,16	0,16	0,16	0,16
0,6	0,20	0,24	0,24	0,24	0,24	0,24	0,24	0,24	0,24
0,8	0,27	0,32	0,32	0,32	0,32	0,32	0,32	0,32	0,33
1,0	0,34	0,40	0,41	0,41	0,41	0,41	0,41	0,41	0,41
1,2	0,41	0,49	0,49	0,49	0,49	0,49	0,49	0,49	0,49

The analytical results are calculated for electromagnetically isolated voltage transformer in Table I and isolated current transformer in Table II. The classical analysis can not be applied for the regime of combined instrument trans-

former because the mutual electromagnetic influence is not possible to be estimated by classical means. However, the FEM-3D analysis is accomplished from plug out regime to 120% of the input voltages and currents of the both measurement cores by taking into account the electromagnetic influence of the cores.

By using the numerical integration the leakage flux of one turn in each of the windings ψ_σ are calculated. The leakage fluxes ψ_σ of the windings are:

$$\psi_\sigma = N \cdot \phi_\sigma \quad (2)$$

where N is the number of winding turns. The leakage inductances L_σ are derived by:

$$L_\sigma = \frac{\psi_\sigma}{I} \quad (3)$$

where I is the winding current.

In figures 4 and 5 the numerically calculated primary and secondary winding leakage inductance dependencies via the input voltage of the voltage measurement core are shown.

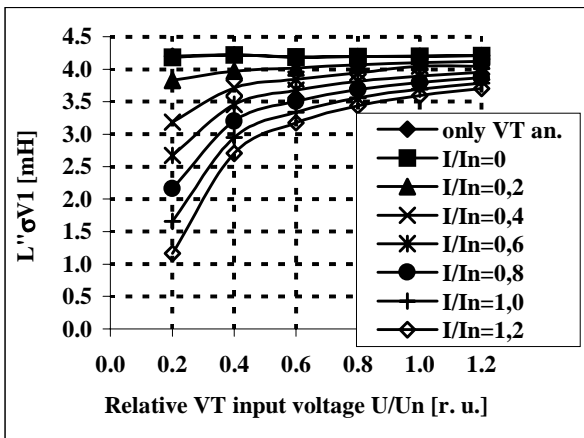


Fig. 4. Leakage inductance $L''_{\sigma V1}$ of the primary VT winding

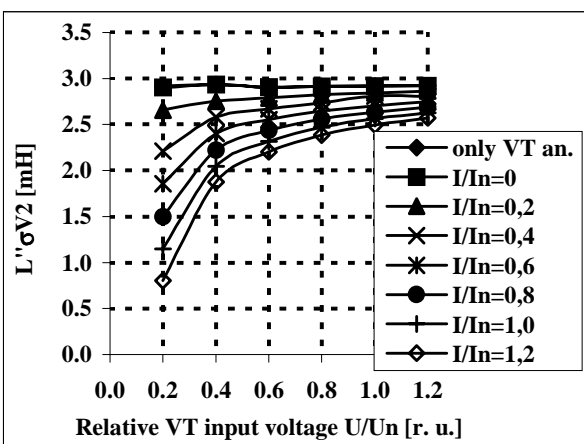


Fig. 5. Leakage inductance $L''_{\sigma V2}$ of the secondary VT winding

In figures 6 and 7 the numerically calculated primary and secondary winding leakage inductance dependencies via

the input current of the current measurement core are displayed.

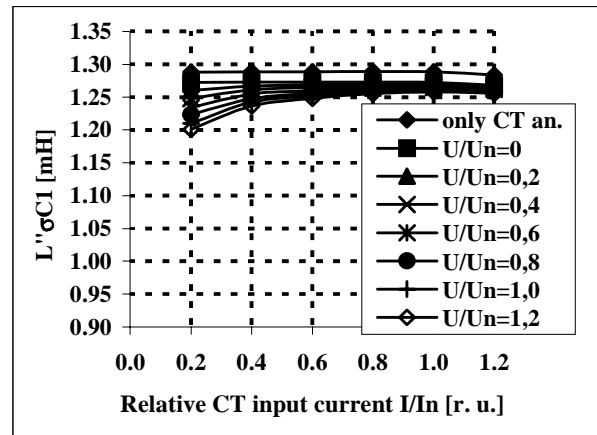


Fig. 6. Leakage inductance $L''_{\sigma C1}$ of the primary CT winding

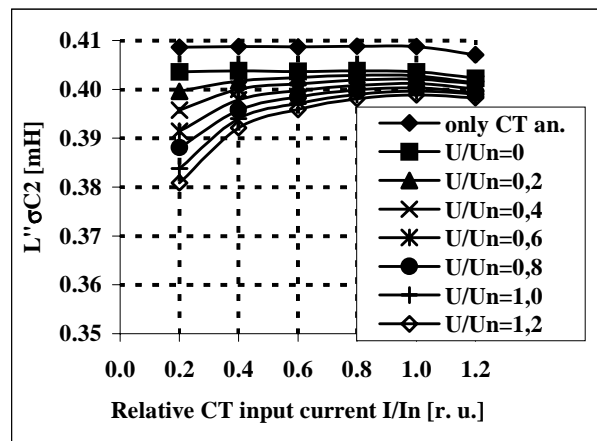


Fig. 7. Leakage inductance $L''_{\sigma C2}$ of the secondary CT winding

4. METROLOGICAL CHARACTERISTICS

The numerically calculated leakage inductances enable further derivation of the winding leakage reactances given in [2]. This leads to the main metrological characteristics of the combined instrument transformer: the voltage, current and phase difference errors.

The voltage error p_u is a sum of the voltage error under no load p_{u0} and the error introduced by the transformer load p_{ul} .

Table III. Voltage error under no load

I/I_n	only VT	0	0,2	0,4	0,6	0,8	1,0	1,2
	numerical							
U/U_n	p_{u0} [%]							
0,2	-0,34	-0,34	-0,31	-0,26	-0,22	-0,18	-0,15	-0,11
0,4	-0,28	-0,28	-0,26	-0,25	-0,23	-0,22	-0,20	-0,19
0,6	-0,24	-0,24	-0,23	-0,23	-0,22	-0,21	-0,20	-0,19
0,8	-0,22	-0,22	-0,22	-0,21	-0,21	-0,20	-0,19	-0,19
1,0	-0,21	-0,21	-0,20	-0,20	-0,20	-0,19	-0,19	-0,18
1,2	-0,21	-0,21	-0,20	-0,20	-0,19	-0,19	-0,19	-0,18

Table IV. Voltage error introduced by the load

I/I_n	only VT	0	0,2	0,4	0,6	0,8	1,0	1,2
	numerical							
U/U_n	p_u [%]							
0,2	-12,35	-12,3	-11,5	-9,91	-8,69	-7,46	-6,26	-5,07
0,4	-6,20	-6,20	-5,90	-5,59	-5,29	-4,98	-4,68	-4,38
0,6	-4,10	-4,10	-3,97	-3,83	-3,70	-3,56	-3,43	-3,30
0,8	-3,08	-3,08	-3,01	-2,93	-2,85	-2,78	-2,70	-2,63
1,0	-2,47	-2,47	-2,42	-2,39	-2,32	-2,27	-2,23	-2,18
1,2	-2,06	-2,06	-2,03	-1,99	-1,96	-1,93	-1,89	-1,86

Table V. Voltage error of the voltage measurement core

I/I_n	only VT	0	0,2	0,4	0,6	0,8	1,0	1,2
	numerical							
U/U_n	p_u [%]							
0,2	-12,69	-12,6	-11,8	-10,2	-8,92	-7,65	-6,41	-5,18
0,4	-6,48	-6,48	-6,16	-5,84	-5,52	-5,20	-4,88	-4,57
0,6	-4,35	-4,35	-4,21	-4,06	-3,92	-3,77	-3,63	-3,49
0,8	-3,31	-3,31	-3,23	-3,15	-3,07	-2,98	-2,90	-2,82
1,0	-2,68	-2,68	-2,63	-2,60	-2,52	-2,47	-2,42	-2,37
1,2	-2,27	-2,27	-2,23	-2,20	-2,16	-2,12	-2,08	-2,05

The phase difference error δ_u of the voltage measurement core is a sum of the phase error under no load δ_{u0} and the phase difference error introduced by the transformer load δ_{ul} .

Table VI. VT phase difference error under no load

I/I_n	only VT	0	0,2	0,4	0,6	0,8	1,0	1,2
	numerical							
U/U_n	δ_{u0} [min]							
0,2	-4,99	-4,96	-4,41	-3,39	-2,59	-1,79	-1,00	-0,22
0,4	-4,77	-4,77	-4,41	-4,04	-3,67	-3,33	-2,94	-2,59
0,6	-4,95	-4,95	-4,70	-4,45	-4,21	-3,90	-3,71	-3,48
0,8	-4,72	-4,72	-4,54	-4,37	-4,19	-4,02	-3,84	-3,68
1,0	-4,48	-4,48	-4,34	-4,27	-4,08	-3,95	-3,82	-3,69
1,2	-4,43	-4,43	-4,32	-4,21	-4,11	-3,99	-3,88	-3,78

Table VII. VT phase difference error introduced by the load

I/I_n	only VT	0	0,2	0,4	0,6	0,8	1,0	1,2
	numerical							
U/U_n	δ_{ul} [min]							
0,2	-407	-405	-366	-295	-240	-183	-128	-73,9
0,4	-205	-205	-191	-177	-163	-149	-135	-121
0,6	-135	-135	-129	-122	-116	-110	-104	-98,3
0,8	-101	-101	-98,3	-94,8	-91,3	-87,8	-84,3	-80,9
1,0	-81,5	-81,5	-79,3	-78,1	-74,8	-72,6	-70,4	-68,2
1,2	-68,1	-68,1	-66,5	-65,0	-63,4	-61,9	-60,3	-58,8

Table VIII. VT Phase difference error

I/I_n	only VT	0	0,2	0,4	0,6	0,8	1,0	1,2
	numerical							
U/U_n	δ_u [min]							
0,2	-412	-410	-371	-299	-242	-185	-129	-74,1
0,4	-209	-209	-195	-181	-166	-152	-138	-124
0,6	-140	-140	-133	-127	-120	-114	-108	-101
0,8	-106	-106	-102	-99,2	-95,5	-91,8	-88,1	-84,6
1,0	-86,0	-86,0	-83,6	-82,4	-78,9	-76,5	-74,2	-71,9
1,2	-72,5	-72,5	-70,8	-69,2	-67,5	-65,9	-64,2	-62,6

In Tables IX. and X. the metrological characteristics of the current measurement core are given.

TABLE IX. Current error of the current measurement core

U/U_n	only CT	0	0,2	0,4	0,6	0,8	1,0	1,2
	numerical							
I/I_n	p_i [%]							
0,2	-1,16	-1,16	-1,16	-1,16	-1,16	-1,16	-1,16	-1,16
0,4	-0,89	-0,89	-0,89	-0,89	-0,89	-0,89	-0,89	-0,89
0,6	-0,75	-0,75	-0,75	-0,75	-0,75	-0,75	-0,75	-0,75
0,8	-0,68	-0,68	-0,68	-0,68	-0,68	-0,68	-0,68	-0,68
1,0	-0,68	-0,68	-0,68	-0,68	-0,68	-0,68	-0,68	-0,68
1,2	-0,64	-0,64	-0,64	-0,64	-0,64	-0,64	-0,64	-0,64

TABLE X. CT phase difference errors

U/U_n	only CT	0	0,2	0,4	0,6	0,8	1,0	1,2
	numerical							
I/I_n	δ_i [min]							
0,2	8,47	8,54	8,59	8,64	8,69	8,74	8,79	8,83
0,4	3,82	3,87	3,89	3,90	3,92	3,95	3,96	3,98
0,6	2,59	2,63	2,64	2,65	2,66	2,67	2,68	2,69
0,8	0,84	0,87	0,88	0,89	0,90	0,90	0,91	0,92
1,0	0,50	0,54	0,54	0,55	0,55	0,56	0,57	0,57
1,2	0,17	0,20	0,21	0,21	0,22	0,23	0,23	0,23

5. CONCLUSIONS

The FEM calculation of the magnetic parameters enables correct calculation of the main combined transformer metrological specifications by taking into account the mutual electromagnetic influence of the two measurement cores. The voltage measurement core is accuracy class 3 and the current measurement core is accuracy class 1. This will enable further optimal design of instrument transformer by using the stochastic optimisation techniques (e. g. genetic algorithm).

REFERENCES

- [1] IEC 60044-3 (1980-01): Instrument Transformers, Part 3: Combined Transformers, 1980.
- [2] M. Cundeve, L. Arsov "Metrologically Improved Design of Combined Current-Voltage Instrument Transformer by Using FEM-3D", *Proc. of 12th IMEKO TC 4 Int. Symp.*, pp.282-285 Zagreb, Croatia, 2002
- [3] M. Cudev, L. Petkovska, V. Stoilkov, G. Cvetkovski "From Macroelements to Finite Elements in 3D-FEM Modelling", *Proc. of FEM3D Int. Conf.*, pp. 5-6 Jyvaskyla, Finland, 2000.
- [4] E. Lesniewska, J. Chojancki "Influence of the Correlated Localisation of Cores and Windings on Measurement Properties of Current Transformers", *Proc. of 10th Int. Symposium on Electromagnetic Fields in Electrical Engineering ISEF 2001* pp. 281-286, Cracow, Poland, 2001.

AUTHOR(S): Marija Cundeve, University "Sts. Cyril & Methodius", Faculty of Electrical Engineering, Karpos II b.b. POBox 574, 1000 Skopje, R. Macedonia, phone: +389 2 399162, fax: +389 2 364262, E-mail: mcundeve@cerera.etf.ukim.edu.mk

Ljupco Arsov, Faculty of Electrical Engineering, Karpos II b.b. POBox 574, 1000 Skopje, R. Macedonia, phone: +389 2 399111, fax: +389 2 364262, E-mail: ljarsov@cerera.etf.ukim.edu.mk